Available online at www.sciencedirect.com

ScienceDirect

Procedia Manufacturing 00 (2019) 000–000

Procedia MANUFACTURING

www.elsevier.com/locate/procedia

47th SME North American Manufacturing Research Conference, NAMRC 47, Pennsylvania, USA

Error qualification for multi-axis BC-type machine tools

Maxwell Praniewicz, Thomas R. Kurfess, Christopher Saldana*

George W. Woodruff School of Mechanical Engineering, Georgia Institute of Technology, 801 Ferst Drive, Atlanta, Georgia 30332

* Corresponding author. *E-mail address:* christopher.saldana@me.gatech.edu

Abstract

Multi-axis machining processes are often used to fabricate complex components with tight geometric tolerances. Thus, the need for highly accurate 5-axis machine tools is imperative in high precision industries such as aerospace and mold and die. Often, construction errors result in geometric errors within the machine tool. These errors must be identified and compensated in order to guarantee accuracy of the machine. In this work, kinematic equations of motion for a BC-style machine tool were derived while incorporating the 8 distinct kinematic error constants associated with a 5-axis machine tool. A method is presented to derive these kinematic error constants from eccentricity values obtained using 3-axis simultaneous tests for table-table style 5-axis machine tools. To validate this method, error constants were input into the kinematic simulation. Eccentricity values were then output from the simulation and error constants were derived and compared to the input values. It was shown that if the procedure is followed, the error constants can be correctly derived and compensated. This method was then implemented on a BC-style machine tool and error constants were derived.

Keywords: machine error compensation; double ballbar; machining

1. Introduction

While the accuracy requirement of a computer numerical control (CNC) machine tool component may change between jobs, typical machined components require feature tolerances on the order of 0.1 mm, which is achievable on a typical machine tool. However, certain industries demand significantly greater accuracy from their CNC machines. Manufacturers of molds and dies, optics, and medical implants require feature accuracies on the order of 10 μm and final surface roughness on the order of 10 nm. Moreover, manufacturers in these industries have turned to multi-axis machine tools to reduce the number of setups for complex parts and increase efficiency.

The accuracy of a machine tool can be affected by several factors: machine tool construction, servo/drive position accuracy, thermal distortion, among others. These errors can be reduced by innovations in machine design, advanced control algorithms, and construction error identification and qualification [1]. The last of these is essential and can be done through measurements performed on the machine tool. Geometric errors in a machine tool can be separated into two categories: position dependent geometric errors (PDEGs) and position independent geometric errors (PIGEs) [2]. The value of a PDEGs will change from position to position within the volume of the machine tool and are often related to construction of individual components of the machine tool. However, PIGEs remain invariant throughout the entire machine volume and are often related to inaccuracies of the machine assembly process. Since PIGEs are invariant, they are often regarded as kinematic error constants which skew the geometry of the machine tool

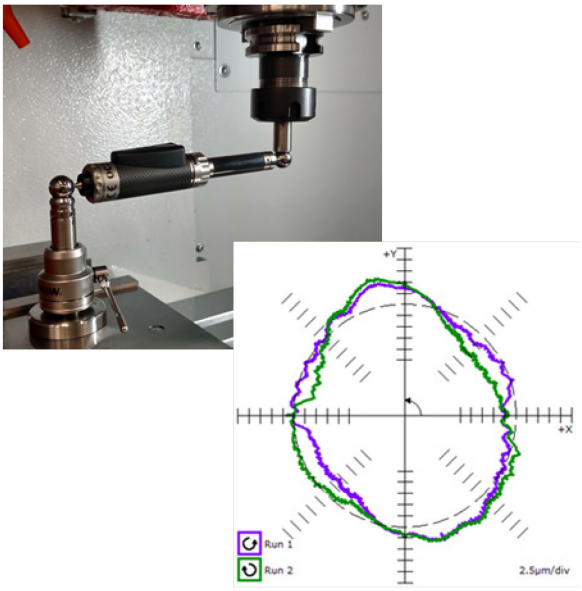

Figure 1: A ballbar setup in a three-axis machine tool and an example result of typical X-Y plane test

from nominal by constant amounts. The path of the machine tool can then be compensated by these error constants to greatly improve the accuracy of the final product [3].

As referenced in the work by Zhang et. al., there are 21 characteristic errors of a three axis machine tool [4]. Six of these errors correspond to each individual axis of movement; positioning error in three orthogonal directions and three angular errors (commonly known as roll, pitch, and yaw). These values are often regarded as PDEGs, since they largely rely on the quality of the guide components along the axis. The final three errors relate to the relative squareness between the individual axes and are often regarded as PIGEs since they are largely affected by the assembly of the axes.

One of the most widely used tools for identification of these errors is the double ballbar. These tools are used to check the roundness of circular paths within the volume of the machine tool. One ball cup is fixed to the table while the other cup is attached to the spindle of the machine tool. The ballbar is then magnetically affixed to these cups by a precision ground sphere at each end. The spindle is moved in an arc within a plane in the volume of the machine. Throughout the arc, the bar measures the variation in radius of this circular path by extending or contracting as the tool moves farther or closer to the fixed base. Figure 1 displays this device installed in a typical three axis machine tool and a typical measurement plot. Standards have been developed to govern how these tests are conducted and the interpretation of their results, making them common measuring devices within industry [5, 6].

Tsutsumi et al. extended the use of these devices into the qualification of 5-axis machine tools which use two rotary axes to change the orientation of the component within the machine tool [7]. Their method used simultaneous movement of three axes, two linear and one rotary, to identify the eight additional error parameters present in a 5-axis machine tool. These eight parameters are comprised of two linear and two angular deviations for each of the rotary axes. The authors then extended their work into simultaneous movement of four axes and required the analysis of only two measurements to characterize all eight parameters [8]. Since these initial works, many others have presented their own methodology for solving these kinematic errors. Wang et al. presented a methodology for determining the kinematic errors which decouples the effects of individual error constants [9]. This method utilized single point measurements of the ballbar rather than utilizing the continuous capture of data.

Others have attempted to utilize only the movement of the rotary axes, thus removing any deviations caused by inaccuracies of the linear position systems. Zhang et al. introduced a method which utilized actuation of only the C rotary axis, but was only able to determine 5 of the necessary error constants [10]. Lei et al. investigated the total dynamic effects of a 5-axis machine tool using ballbar measurements [11]. Their work examined the dynamic interaction of the rotary and linear axes by pairing axes to tune the velocity gains within the machine tool controller. Xiang et al. also introduced an experimental method and analysis which utilizes only rotary axis actuation to characterize the 5-axis kinematic error constants [12]. This method eliminates the need for actuation of the linear axes, However, this method is prone to setup errors which must be carefully characterized and compensated. Lee et al. introduced a device to minimize the runout of the ball which is attached to the spindle, thus greatly reducing the effect of setup error on the measurement process [13].

However, in previous literature there are few examples of machine kinematics and methods for the derivation of error constants for machine configurations other than the AC-type table-table 5-axis machines. This work presents a derivation for BC-style table-table 5-axis machine tool kinematics which incorporates the kinematic error constants associated with the rotary axes. A derivation for these constants is also presented using the eccentricity data obtained from 5-axis ballbar tests. Simulations with input error constants are developed and output eccentricity values are used to derive the original kinematic error constants to validate the performance of the methodology. Finally, the implementation of this method on a BC-style machine tool is discussed.

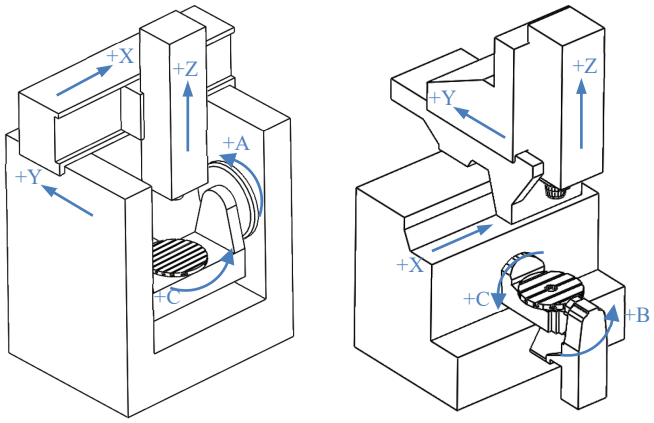

Figure 2: AC and BC 5-axis machine tool configurations

2. Methodology

The structure of the BC-type 5-axis machine tool is shown in Figure 2 as shown in contrast to the AC-type machine. These structures differ in the orientation of the rotary axis which is directly connected to the machine tool base. While the kinematic chain of the three translational axes may change based on machine construction, this work assumes that any errors associated with linear position are negligible. Therefore, the order these axes occur in the kinematic chain is irrelevant and the kinematics can be combined into a single linear positional move in three-dimensional space.

2.1. Machine Kinematic Derivations

Figure 3 depicts the error constants associated with the rotary axes of the BC kinematic configuration. Beginning at the base of the machine, there are two positional deviations, δ_{BX} and δ_{BZ}, which could shift the location of the B axis within the X-Z plane. There are also two angular errors which could change the direction of the axis vector in space. Angle β_B represents a rotation of the B axis about the $\hat{\imath}$ direction in space, while angle γ_B represents a rotation of the B axis about the $\hat{k}$ direction. The location of the C axis center of rotation can also be shifted in with in the X-Y plane and can be represented as parameters δ_{CX} and δ_{CY}. The orientation of this axis in space can also differ from the intended direction and can be represented by two angular deviations. The first, α_B, represents an angle of rotation about the $\hat{\jmath}$ direction. The final term, β_C, represents and angle of rotation about the $\hat{\imath}$ direction.

Using four independent ballbar tests, these constants can be determined. The tests used in this work are the B radial, B axial, C radial, and C axial methods described in [7]. For a given ballbar test, the distance between the table cup and the spindle cup should remain the nominal length of the ballbar L_b, assuming no error. Therefore, the error in the ballbar can be characterized by the spindle position, P_S, the table position P_T, and L_b:

$$dL = L_b - |P_S - P_T| \tag{1}$$

Since we assume that no positioning errors occur in the linear axes, the spindle position will follow the desired circular trajectory at some radius from the center of axis rotation. This radius will change based on whether we are performing an axial or radial test, as this changes the position of the spindle cup relative to the table cup. Thus, the radius of the table cup from the center of rotation will also affect the location of the spindle. In these tests, the table cup is placed along the nominal location in X of the B axis, which eliminates the X component of the radius calculation. For the B axis, this radius will be defined as R_B and denotes the distance in the $\hat{k}$ of the table cup from the nominal position of the B axis. For the C axis, this radius will be defined as R_C and denotes the distance in the $\hat{\jmath}$ direction of the table cup to the table center of rotation. Therefore, the nominal position of the table cup can be defined as:

$$P_N = \begin{bmatrix} 0 \\ R_C \\ R_B \end{bmatrix} \tag{2}$$

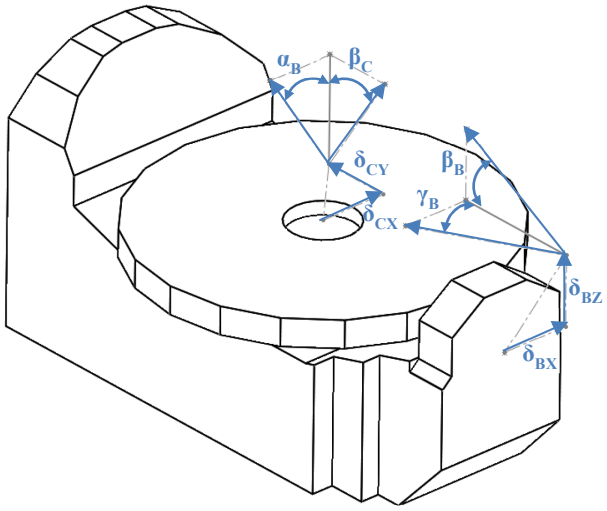

Figure 3: Kinematic error terms associated with the BC type machine tool

The position of the spindle can then be written as a function of the angle of rotation of either the B or C axis and the spindle offset for the test being performed, which is defined as φ and θ, respectively:

$$P_S = R_Z(\theta)R_Y(\varphi)[P_N + \Delta_S] \tag{3}$$

In Eq. 3, R_Z and R_Y are defined as simple rotations about the Z and Y axes:

$$R_z(\theta) = \begin{bmatrix} \cos(\theta) & -\sin(\theta) & 0 \\ \sin(\theta) & \cos(\theta) & 0 \\ 0 & 0 & 1 \end{bmatrix} \tag{4}$$

$$R_Y(\varphi) = \begin{bmatrix} \cos(\varphi) & 0 & \sin(\varphi) \\ 0 & 1 & 0 \\ -\sin(\varphi) & 0 & \cos(\varphi) \end{bmatrix} \tag{5}$$

Note that in the case of the ballbar tests, only one rotational axis will be used at once, while keeping the other constant at zero. The spindle offset will also change based on the test performed. For the B radial and C axial tests, the offset occurs in the $\hat{k}$ direction (Eq. 6), while in the B axial and C radial tests the offset occurs in the $\hat{\jmath}$ direction (Eq. 7):

$$\Delta_S = \begin{bmatrix} 0 \\ 0 \\ L_b \end{bmatrix} \tag{6}$$

$$\Delta_S = \begin{bmatrix} 0 \\ L_b \\ 0 \end{bmatrix} \tag{7}$$

The table cup position, P_T, must also be written as a function of φ and θ while incorporating the kinematic error constants. The form of P_T can generally be expressed as:

$$P_T = T_B T_C + \Delta L_B \tag{8}$$

In Eq. 8, T_B and T_C generally represent the B and C rotary transformations, respectively and ΔL_B represents the linear deviations of the B axis. ΔL_B can be represented simply as:

$$\Delta L_B = \begin{bmatrix} \delta_{BX} \\ 0 \\ \delta_{BZ} \end{bmatrix} \tag{9}$$

T_B can be defined as the combination of angular errors

associated with the B axis, as well as the rotation of the B axis itself. Since the error α_B acts in the same direction as the rotation of B, it can be included as a static rotational offset. Thus, T_B can be defined:

$$T_B = \Delta_{\beta_B}\Delta_{\gamma_B}R_B(\theta) \tag{10}$$

where Δ_{β_B}, Δ_B, and R_B are defined as:

$$\Delta_{\beta_B} = \begin{bmatrix} 1 & 0 & 0 \\ 0 & \cos(\beta_B) & -\sin(\beta_B) \\ 0 & \sin(\beta_B) & \cos(\beta_B) \end{bmatrix} \tag{11}$$

$$\Delta_{\gamma_B} = \begin{bmatrix} \cos(\gamma_B) & -\sin(\gamma_B) & 0 \\ \sin(\gamma_B) & \cos(\gamma_B) & 0 \\ 0 & 0 & 1 \end{bmatrix} \tag{12}$$

$$R_B(\theta) = \begin{bmatrix} \cos(\varphi+\alpha_B) & 0 & \sin(\varphi+\alpha_B) \\ 0 & 1 & 0 \\ -\sin(\varphi+\alpha_B) & 0 & \cos(\varphi+\alpha_B) \end{bmatrix} \tag{13}$$

T_C includes angular deviations associated with the C axis, and must also include the linear deviations of the C axis and the rotation angle θ:

$$T_C = \Delta_{\beta_C}R_C(\theta)P_N + \Delta L_C \tag{14}$$

The terms in Eq. 14, with the exception of P_N defined in Eq. 2, are defined as:

$$\Delta_{\beta_C} = \begin{bmatrix} 1 & 0 & 0 \\ 0 & \cos(\beta_C) & -\sin(\beta_C) \\ 0 & \sin(\beta_C) & \cos(\beta_C) \end{bmatrix} \tag{15}$$

$$R_C(\theta) = \begin{bmatrix} \cos(\theta) & -\sin(\theta) & 0 \\ \sin(\theta) & \cos(\theta) & 0 \\ 0 & 0 & 1 \end{bmatrix} \tag{16}$$

$$\Delta L_C = \begin{bmatrix} \delta_{CX} \\ \delta_{CY} \\ 0 \end{bmatrix} \tag{17}$$

By altering φ and θ, simulations can be performed using input error constants and testing parameters. This is valuable for verification of ballbar results and estimation of positional deviation give specific error parameters.

2.2. Machine Kinematic Derivations

For the identification of errors in the ballbar tests, calculated eccentricity values from the individual tests can be used to systematically determine the kinematic error constants. This procedure was determined in a similar manner as listed in Ref. [7].

First, the B radial test will yield eccentricity values within the X-Z plane defined as B_{rX} and B_{rZ}. Assuming that angular deviations are small, any eccentricity seen can be related to the eccentricity of the B axis. Thus, the linear deviations in the B axis can be calculated:

$$\delta_{BX} = -B_{rX} \tag{18}$$

$$\delta_{BZ} = -B_{rZ} \tag{19}$$

Next, the B axial test will again provide eccentricity values within the X-Z plane that are defined as B_{aX} and B_{aZ}. These values can then be used to determine the angular deviations associated with the B axis:

$$\gamma_B = \sin^{-1}\frac{-B_{aX}}{R_B} \tag{20}$$

$$\beta_B = \sin^{-1}\frac{B_{aZ}}{R_B} \tag{21}$$

In the C axial test, eccentricity values C_{aX} and C_{aY} are found in the X-Y plane. Using these values and β_B calculated in Eq. 21, the angular deviations associated with the C axis can be calculated as:

$$\alpha_B = \sin^{-1}\frac{C_{aX}}{R_C} \tag{22}$$

$$\beta_C = \sin^{-1}\left(-\frac{C_{ay}}{R_C} - \sin\beta_B\right) \tag{23}$$

Finally, in the C radial test, eccentricity values C_{rX} and C_{rY} are found in the X-Y plane. Using values calculated previously, the linear deviations associated with the C can be calculated:

$$\delta_{CX} = -\delta_{BX} - C_{rX} - R_b\sin\alpha_B \tag{24}$$

$$\delta_{CY} = -C_{rY} + R_B\sin\beta_C + R_B\sin\beta_B \tag{25}$$

This method can then be used to determine the kinematic error constants associated with the rotary axes using eccentricity data extracted from the ballbar results.

3. Results

In order to validate the simplifications made to construct the error constant equations, simulations were performed using the derived machine kinematics equations. The B axis tests were simulated between 0° and -90° and the C axis tests were simulated from 0° to 360°. The simulation input parameters, including the table cup position and the kinematic error constants are listed in Table 1. 2121

Table 1: Parameters used in BC simulations

Input Parameter	Value
L_b	150 mm
R_B	175 mm
R_C	100 mm
δ_{BX}	0.010 mm
δ_{BZ}	0.025 mm
δ_{CX}	-0.025 mm
δ_{CY}	-0.010 mm
α_B	-0.0025°
β_B	0.005°
γ_B	0.0025°
β_C	-0.005°

The results from these simulations can be seen in Figure 4, which shows the nominal path of the simulated travel in black and the simulated result using the error constants in blue. For each of the four tests completed, eccentricities of the resultant path were determined by fitting circle segments to each and calculating the deviation between the fit and nominal arc centers. These resulting values are also displayed in each of the corresponding plots in Figure 4.

In order to evaluate the ability of the identification

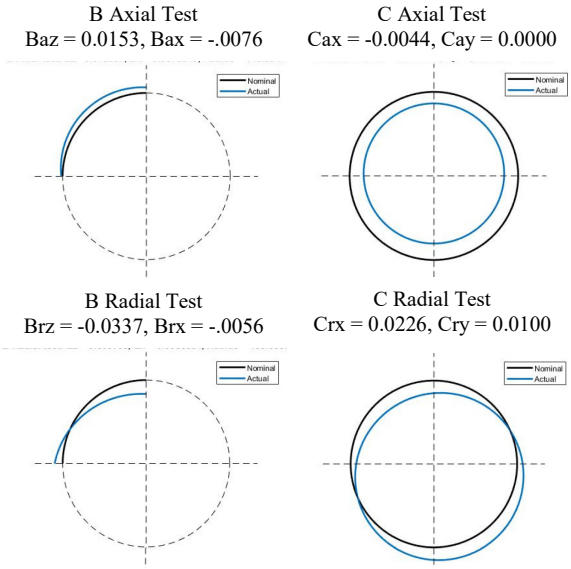

Figure 4: Simulation results with input parameters with deviations (magnified by 1000x)

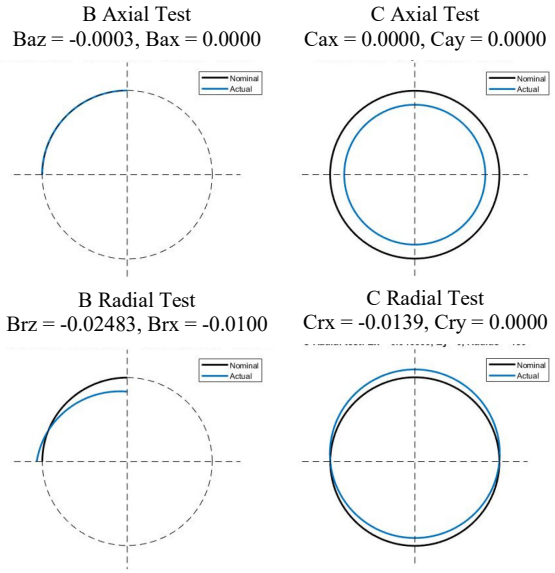

Figure 5: Simulation results with compensated error constants (magnified by 1000x)

equations to correctly derive the error parameters from the eccentricity values reported in the four ballbar tests, these simulated values were then input in Eq. 18 through Eq. 25, along with the R_B and R_C values used in the simulation. The output error parameters were then reported and compared to the originally input values.

The output error values from this test are shown in Table 2 along with the deviation from the value input in the original simulation. These results show that the error constant calculation is able to successfully derive the angular deviations from the eccentricity data. The linear deviations in the C are also calculated fairly accurately. However, in the calculations for the B axis linear deviations, this method appears to be limited. This is most likely due to the simple assumption made in the first step of calculation.

In order to mitigate these effects, the machine controller can be compensated for the angular deviations and the C axis linear deviations. Then if the tests are executed again, the angular deviations should no longer have an effect on the outcome of the B radial test. To test this, the error constants in the simulation were compensated by the calculated error constant with the exception of the B axis linear values. The simulation was then run once again to determine the eccentricity values. These values were then input into the error constant calculation to determine the final machine errors.

Figure 5 shows the result of these final simulations and displays the calculated eccentricity values. For each of the four tests shown, the compensation is shown to reduce the concentricity error of the resultant path. For both of the axial tests, the error is reduced almost completely. Both radial tests still show residual errors, but both have been reduced in magnitude, with the exception of the B_{rX} error.

These new eccentricity values were then input into the error constant calculation. Table 3 displays the output error constants from these calculations. The angular deviations calculated from the simulation all show negligible error, which agrees with the compensation added from the previous test. While some compensation was added for the linear deviations of the C axis, deviations did still exist. In the second simulation, these errors were correctly identified. Most importantly, the imposed linear deviations on the B axis have now been correctly identified, resulting in a fully identified system. These results have shown that by implementing the proper compensation procedure, the error detection algorithm is capable of correctly identifying kinematic errors of a BC-style 5-axis machine tool.

4. Discussion

For further investigation, this error measurement procedure was implemented on a BC-style 5-axis machine (Mazak VCU-500) shown in Figure 6. For simplicity of controlling the process within the limits of this machine, measurement limits of all four tests were changed. In B axis tests, the range of φ was set to begin at 35° and end at -55°. For C axis tests, the

Table 2: Output of error constant calculation – initial

Output Parameters	Value	Deviation
δ_{BX}	0.0056 mm	-0.0044 mm
δ_{BZ}	0.0337 mm	0.0117 mm
δ_{CX}	-0.0206 mm	0.0040 mm
δ_{CY}	-0.0100 mm	0.0000 mm
α_B	-0.0025°	0.0000°
β_B	0.0049°	-0.0001°
γ_B	0.00249°	-0.00001°
β_C	-0.0049°	0.0001°

Table 3: Output of error constant calculation - final

Output Parameters	Value	Deviation
δ_{BX}	0.0100 mm	0.0000 mm
δ_{BZ}	0.0248 mm	-0.0002 mm
δ_{CX}	0.0039 mm	-0.0001 mm
δ_{CY}	0.0000 mm	0.0000 mm
α_B	0.0000°	0.0000°
β_B	0.00009°	0.00009°
γ_B	0.0000°	0.0000°
β_C	0.0000°	0.0000°

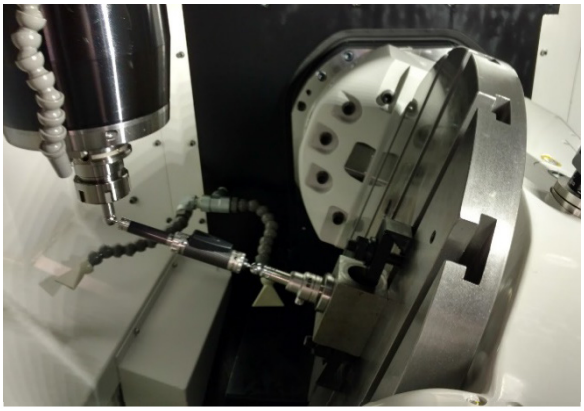

Figure 6: B radial test within a BC style 5-axis machine tool

range of θ was set to begin at 110° and end at 260°. However, changing the limits of the test should not affect the results as these are still viable ranges from which eccentricity values can be calculated.

A Renishaw QC20-W ballbar was used in the measurements. The ballbar was calibrated between each test with a measurement uncertainty of 0.1 µm, was run at a nominal feed rate of 1000 mm/min, and captured data at a sampling rate of 26.3 Hz. Using the nominal locations for the center of rotation for both the B and C axes which are provided in parameters of the machine controller, the table cup was positioned in X along the B rotational axis. The table cup location was then recorded and R_B and R_C were calculated to be 178.250 mm and 97.847 mm, respectively. L_b, the nominal ballbar length, used for these tests was 150 mm.

Eccentricity values for each test were calculated and plots for each were saved for comparison. Eccentricity results were input into the kinematic error constant calculations. For the sake of verification, the derived error constants and testing parameters were also input for simulation. The resulting simulated paths were then compared to the measured plots to ensure agreement between the two systems.

Table 4 shows the derived error constants for this set of machine tool tests. These constants show significant error in the linear and angular deviations of both rotary axes. If left uncompensated, these could cause significant deviations in a simultaneous 5-axis machining operation. Across a table diameter of 500 mm, an angular deviation of 0.0127° could result in a positioning error of up to 0.1108 mm. Combined with the linear deviations seen, the expected error could surpass 0.14 mm, which for high precision components typically produced on a 5-axis machining center is unacceptable.

Table 4: Derived error constants from machine tool test

Input Parameter	Value
δ_{BX}	0.0185 mm
δ_{BZ}	0.0244 mm
δ_{CX}	-0.0529 mm
δ_{CY}	-0.0325 mm
α_B	-0.0040°
β_B	0.0127°
γ_B	-0.0003°
β_C	-0.0108°

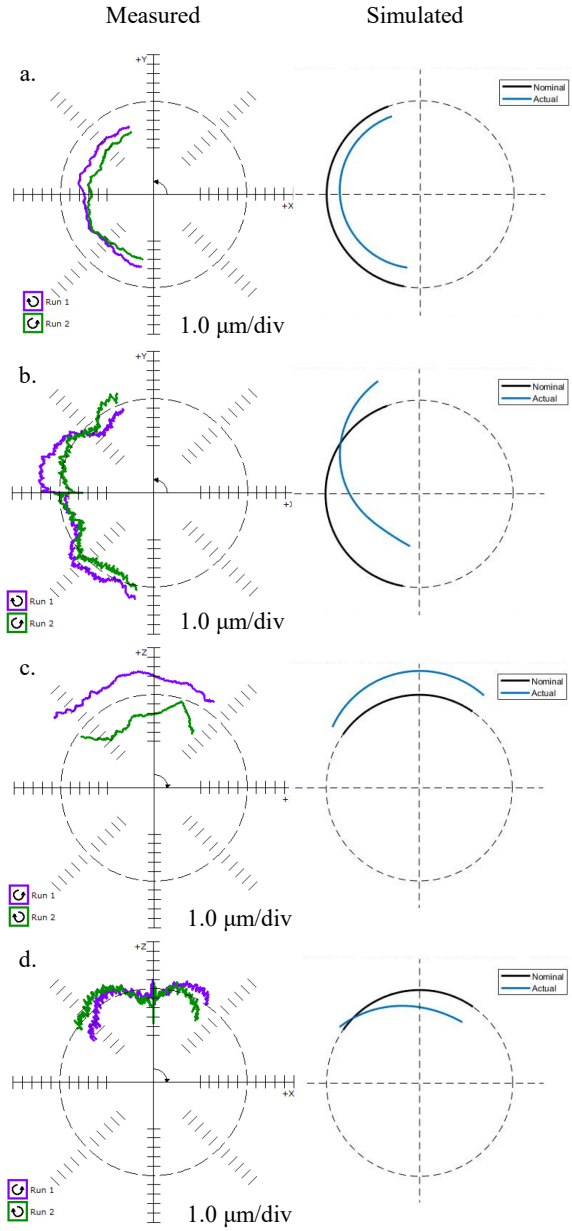

Figure 7: Comparison of ballbar measurements to simulations using the derived error constants. (a.) C axial (b,) C radial (c.) B axial (d.) B radial

However, by directly comparing the measurement data to the simulation, significant differences can be seen in the paths, as shown in Figure 7. By inspection, the measured deviation does not necessarily follow the expected circular arc. Because of this, the fit performed and the derived arc centers may not accurately represent the plot. In both radial measurements, the form observed is only slightly circular. Thus, the eccentricity values and the derived error constants may not necessarily accurately depict the phenomena observed. This can be seen in the simulations of each of these tests. For both of the radial tests, the simulation does not appear to closely follow the measured results. However, in the axial tests the simulations do appear to follow the measured results.

If the measurement noise and form error were to be reduced, these tests show that the kinematic model and the derivation of error constants appear to be consistent with measurements acquired from tests. Proprietary control of machine parameters made it not possible to compensate the rotary axes in the

present work. Future work would be include verification of the accuracy of these derived parameters through access to machine parameters or execution on a compatible controller. Further, these tests could be verified using artificial compensation within the programed path.

5. Conclusions

In this work, kinematic equations of motion for a BC-style machine tool were derived while incorporating the 8 distinct kinematic error constants associated with a 5-axis machine tool. A method was then presented to derive these kinematic error constants from eccentricity values obtained using 3-axis simultaneous tests for table-table style 5-axis machine tools using a double ballbar. To validate this method, error constants were input into the kinematic simulation and eccentricity values were then output from the simulation, and error constants were derived and compared to the input values. It was shown that using the procedure, error constants can be correctly derived and compensated. This method was then implemented on a BC-style machine tool and error constants derived. Future work will involve compensation of these errors and investigation of the effect of sensor noise and form error on the derivation of accurate eccentricity values.

Acknowledgement

The authors would like to acknowledge partial support from the National Physical Sciences Consortium (NPSC) for fellowship support for M. Praniewicz. This work was also partially supported by NSF CMMI-1646013, CMMI-1825640 and IIP-1631803.

References

[1] W. Zhu, Z. Wang, and K. Yamazaki, "Machine tool component error extraction and error compensation by incorporating statistical analysis," *International Journal of Machine Tools and Manufacture,* vol. 50, no. 9, pp. 798-806, 2010.

[2] Y. Abbaszadeh-Mir, J. R. R. Mayer, G. Cloutier, and C. Fortin, "Theory and simulation for the identification of the link geometric errors for a five-axis machine tool using a telescoping magnetic ball-bar," (in English), *International Journal of Production Research,* vol. 40, no. 18, pp. 4781-4797, Dec 15 2002.

[3] R. Ramesh, M. Mannan, and A. Poo, "Error compensation in machine tools—a review: part I: geometric, cutting-force induced and fixture-dependent errors," *International Journal of Machine Tools and Manufacture,* vol. 40, no. 9, pp. 1235-1256, 2000.

[4] G. Zhang, R. Ouyang, B. Lu, R. Hocken, R. Veale, and A. Donmez, "A displacement method for machine geometry calibration," *CIRP Annals-Manufacturing Technology,* vol. 37, no. 1, pp. 515-518, 1988.

[5] *ISO 10791-6:2014 Test conditions for machining centres -- Part 6: Accuracy of speeds and interpolations*, 2014.

[6] *ISO 230-4:2005 Test code for machine tools -- Part 4: Circular tests for numerically controlled machine tools*, 2005.

[7] M. Tsutsumi and A. Saito, "Identification and compensation of systematic deviations particular to 5-axis machining centers," (in English), *International Journal of Machine Tools & Manufacture,* vol. 43, no. 8, pp. 771-780, Jun 2003.

[8] M. Tsutsumi and A. Saito, "Identification of angular and positional deviations inherent to 5-axis machining centers with a tilting-rotary table by simultaneous four-axis control movements," (in English), *International Journal of Machine Tools & Manufacture,* vol. 44, no. 12-13, pp. 1333-1342, Oct 2004.

[9] M. Wang, J. Hu, and T. Zan, "Kinematic error separation on five-axis NC machine tool based on telescoping double ball bar," *Frontiers of Mechanical Engineering in China,* vol. 5, no. 4, pp. 431-437, 2010.

[10] Y. Zhang, J. G. Yang, and K. Zhang, "Geometric error measurement and compensation for the rotary table of five-axis machine tool with double ballbar," (in English), *International Journal of Advanced Manufacturing Technology,* vol. 65, no. 1-4, pp. 275-281, Mar 2013.

[11] W. T. Lei, I. M. Paung, and C. C. Yu, "Total ballbar dynamic tests for five-axis CNC machine tools," (in English), *International Journal of Machine Tools & Manufacture,* vol. 49, no. 6, pp. 488-499, May 2009.

[12] S. T. Xiang, J. G. Yang, and Y. Zhang, "Using a double ball bar to identify position-independent geometric errors on the rotary axes of five-axis machine tools," (in English), *International Journal of Advanced Manufacturing Technology,* vol. 70, no. 9-12, pp. 2071-2082, Feb 2014.

[13] K. I. Lee and S. H. Yang, "Robust measurement method and uncertainty analysis for position-independent geometric errors of a rotary axis using a double ball-bar," (in English), *International Journal of Precision Engineering and Manufacturing,* vol. 14, no. 2, pp. 231-239, Feb 2013.